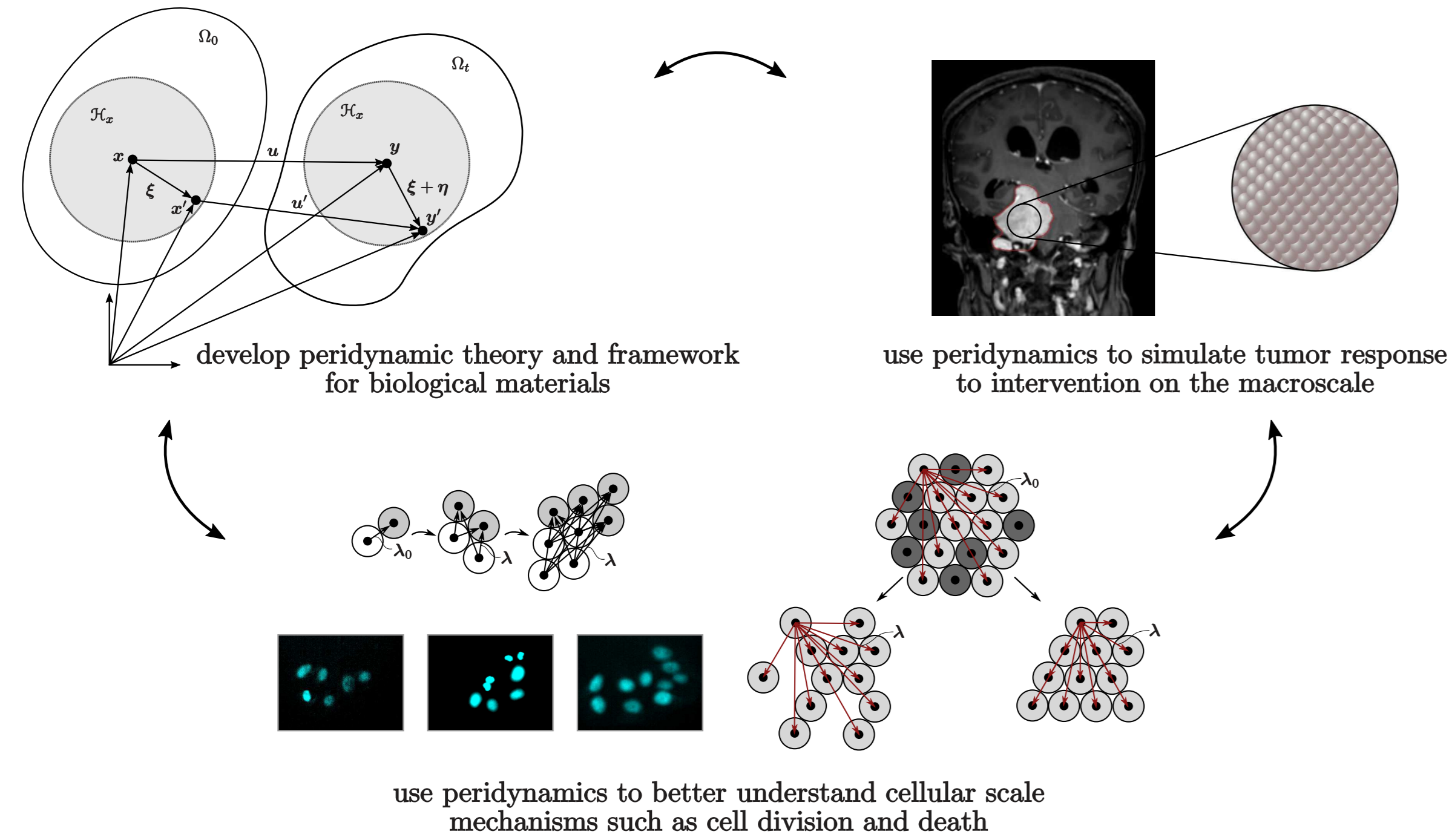


Introduction



- A better understanding of the mechanics of tumor growth and shrinkage could help guide clinical decisions, particularly when tumors are in high-stakes regions.
- We develop a computational framework using **peridynamics** designed to capture cell division as the microscopic mechanism driving tumor growth, and cell death as the microscopic mechanism driving tumor shrinkage.
- As a starting point, we can use this model to study how algorithmic rules and mechanisms applied on cellular scale influence macroscale population or tissue behavior.

Computational Framework

Peridynamic theory is an alternative to classical continuum mechanics where the equation of motion is formulated using integral equations rather than displacement derivatives. In dual-horizon peridynamics, the starting point for this framework, the balance equation at each point \mathbf{x} is formulated based on the horizon $\mathcal{H}_{\mathbf{x}}$ and dual horizon $\mathcal{H}_{\mathbf{x}'}^*$. The equation of motion is

$$\rho \ddot{\mathbf{u}}(\mathbf{x}, t) = \int_{\mathcal{H}_{\mathbf{x}}} \mathbf{f}_{\mathbf{x}\mathbf{x}'}^*(\mathbf{y}, \mathbf{y}') dV_{\mathbf{x}'} - \int_{\mathcal{H}_{\mathbf{x}'}^*} \mathbf{f}_{\mathbf{x}'\mathbf{x}}^*(\mathbf{y}', \mathbf{y}) dV_{\mathbf{x}'} + \mathbf{b}(\mathbf{x}, t).$$

The strain energy density of a growing linear elastic peridynamic solid is written as

$$W(\theta^*, \underline{\underline{e}}^{d*}) = \frac{\kappa \theta^{*2}}{2} + \frac{n(n+2)\mu}{2m_j^*} (\underline{\underline{\omega}}^* \langle \underline{\underline{e}}^{d*} \rangle \cdot \underline{\underline{e}}^{d*}) \quad \|\xi_{jk}^*\| = (1+g_j)r_j + (1+g_k)r_k$$

where growth can be implemented in the constitutive law by modifying this equation such that growth parameter g enters into W and subsequently the peridynamic force density term \mathbf{f} :

$$\underline{\underline{t}}^* = \frac{\partial W^*}{\partial \underline{\underline{e}}^*} \quad \underline{\underline{t}}_{kj}^* \langle \xi_{jk}^* \rangle = \frac{n\kappa\theta_j^*}{m_j^*} \underline{\underline{\omega}}^* \langle \xi_{jk}^* \rangle \|\xi_{jk}^*\| + \frac{n(n+2)\mu}{m_j^*} \underline{\underline{\omega}}^* \langle \xi_{jk}^* \rangle \underline{\underline{e}}^{d*} \langle \xi_{jk}^* \rangle$$

$$\mathbf{f}_{jk}^*(\mathbf{y}_j, \mathbf{y}_k) = \underline{\underline{t}}_{jk}^* \cdot \frac{\mathbf{y}_k - \mathbf{y}_j}{\|\mathbf{y}_k - \mathbf{y}_j\|} \quad \mathbf{f}_{kj}^*(\mathbf{y}_j, \mathbf{y}_k) = \underline{\underline{t}}_{kj}^* \cdot \frac{-(\mathbf{y}_k - \mathbf{y}_j)}{\|\mathbf{y}_k - \mathbf{y}_j\|}$$

When implemented as a meshfree method, it is straight forward to implement algorithmic rules to describe cellular scale mechanisms, for example cell division. Because these rules are often stochastic, many simulations are required to interpret results. We describe average simulation results through tools such as an approximate deformation gradient \mathbf{F} computed by tracking the position of stretch vectors λ between nodes over the course of the simulation $\mathbf{F}\Lambda_0 = \Lambda \Rightarrow \mathbf{F} = \Lambda\Lambda_0^T(\Lambda_0\Lambda_0^T)^{-1}$.

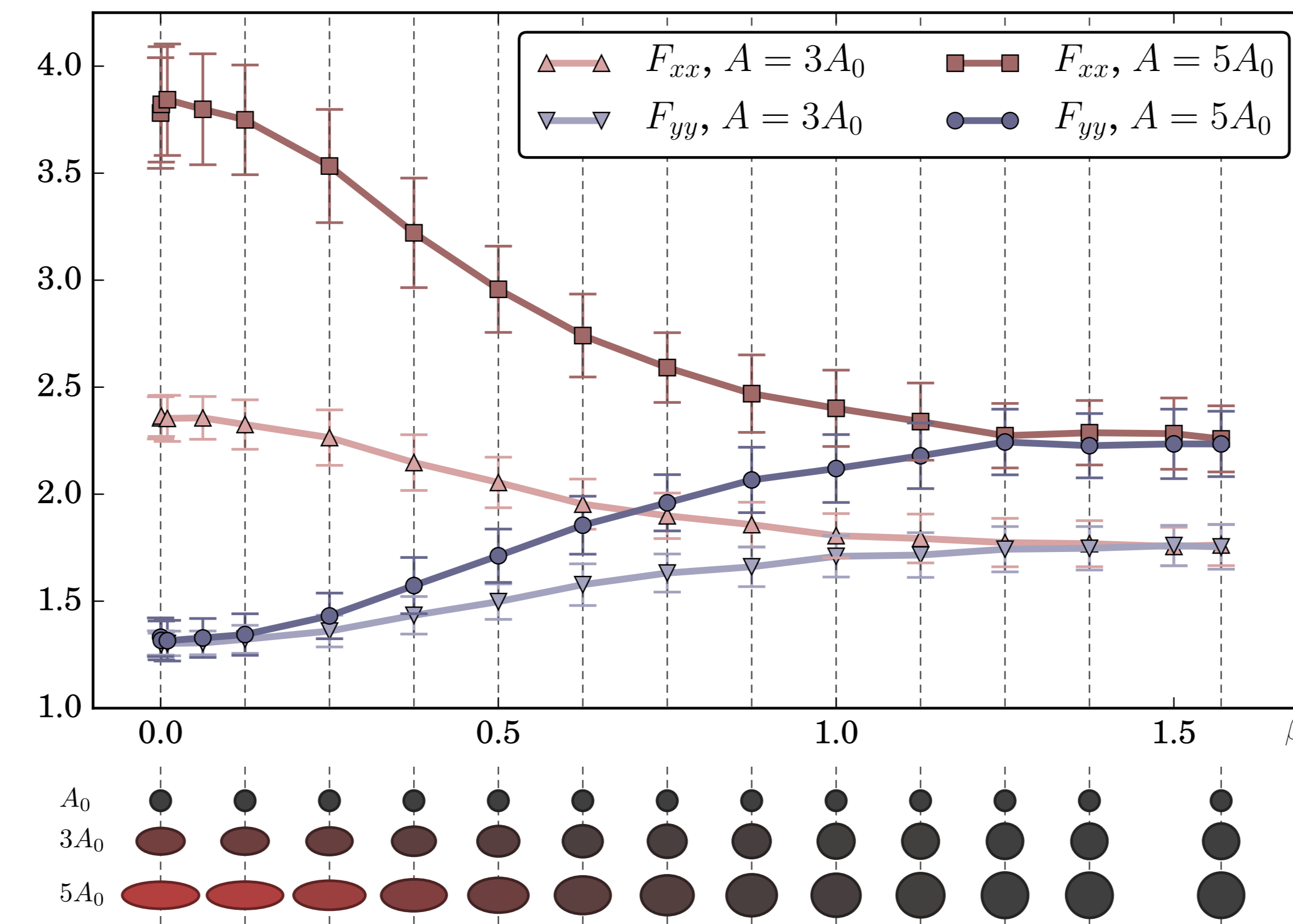
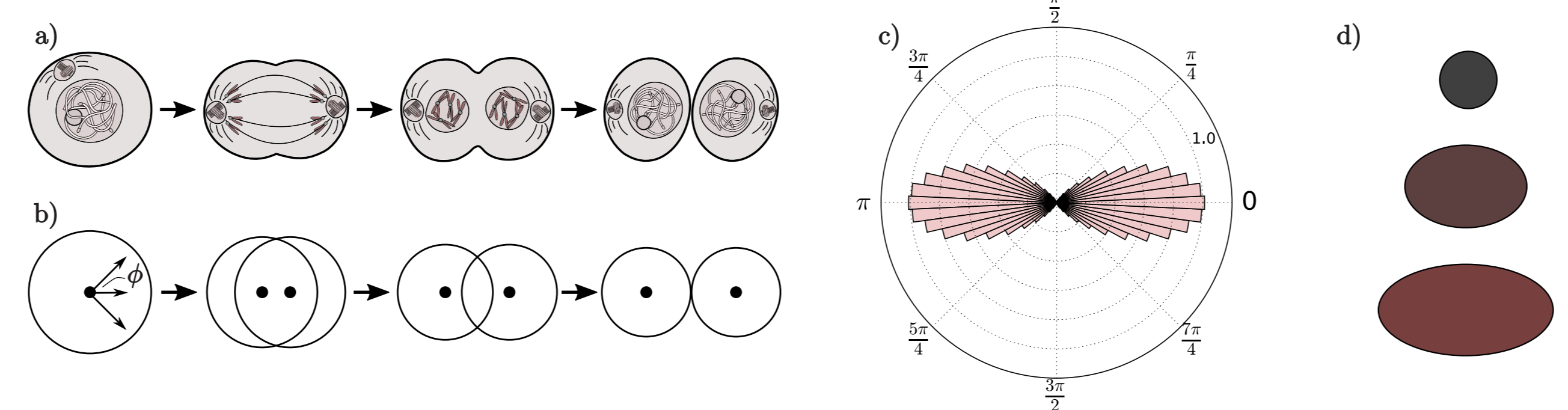
References

- [1] S. A. Silling et al. (2007). *J. Elast.* 88(2):151-184.
- [2] E. Lejeune et al. (2016). *Soft Matter* 12(25):5613-5620.
- [3] E. Lejeune & C. Linder (2017). *Biomech Model Mechanobiol.* 16(4):1141-1157.
- [4] E. Lejeune & C. Linder (2017). *J. Theor. Biol.* 418:1-7.
- [5] E. Lejeune & C. Linder (2018). *J. Theor. Biol.* 73:9-17.
- [6] E. Lejeune & C. Linder (2018). *Biomech Model Mechanobiol.* 17(3):727-743.
- [7] E. Lejeune et al. (2019). *Soft Matter* 15(10):2204-2215.
- [8] E. Lejeune & C. Linder (2020). *CMAME* 360:112700.

Results

Oriented cell proliferation

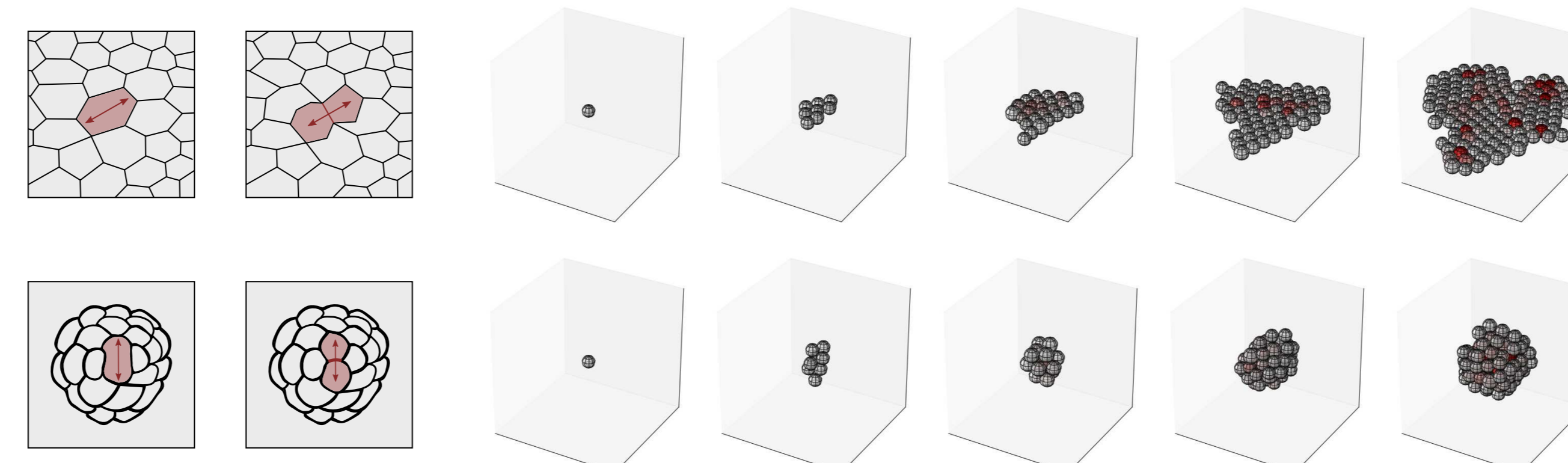
Factors such as cell elongation, local tension, and chemical signaling have all been proposed as mechanisms that control the orientation of cell division. At one extreme, uniformly random cell division corresponds to macroscale isotropic growth. At the other extreme, uniformly polarized cell division will result in macroscale anisotropic growth.



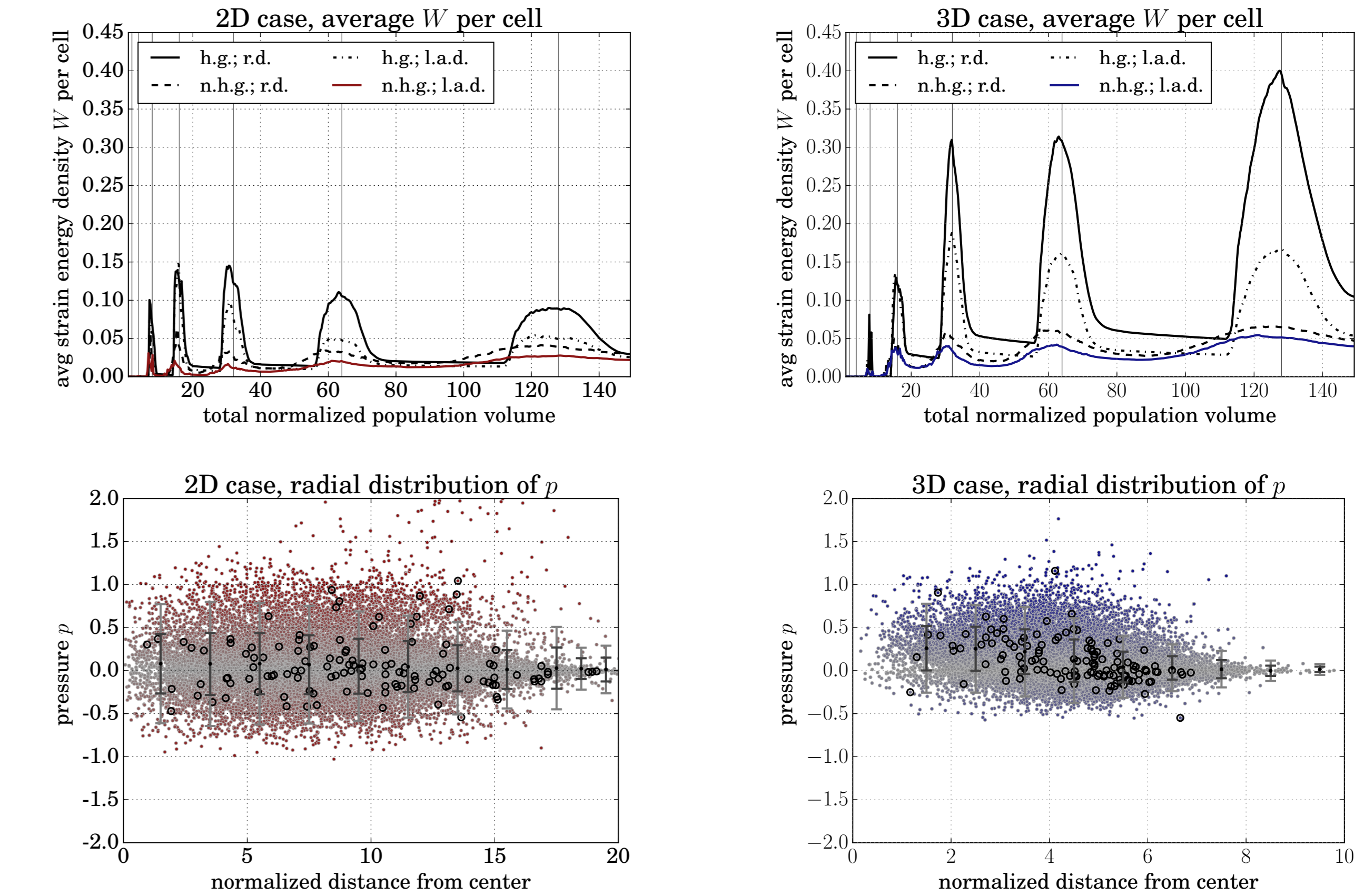
Division angle is defined as $\phi = 0.0 + \beta N(0, 1)$ and F_{xx}, F_{yy} are plotted with respect to β . Each point on the graph represents the mean of 200 simulations. The ellipses are used to visualize average population morphology.

Cell proliferation in monolayers and spheroids

For naturally spherical cells, the longest axis corresponds to the direction of maximum principle stress. If cells always divide perpendicular to their longest axis, less stress will accumulate in the growing material. This rule can be applied for proliferating monolayers (two-dimensional) and spheroids (three-dimensional).

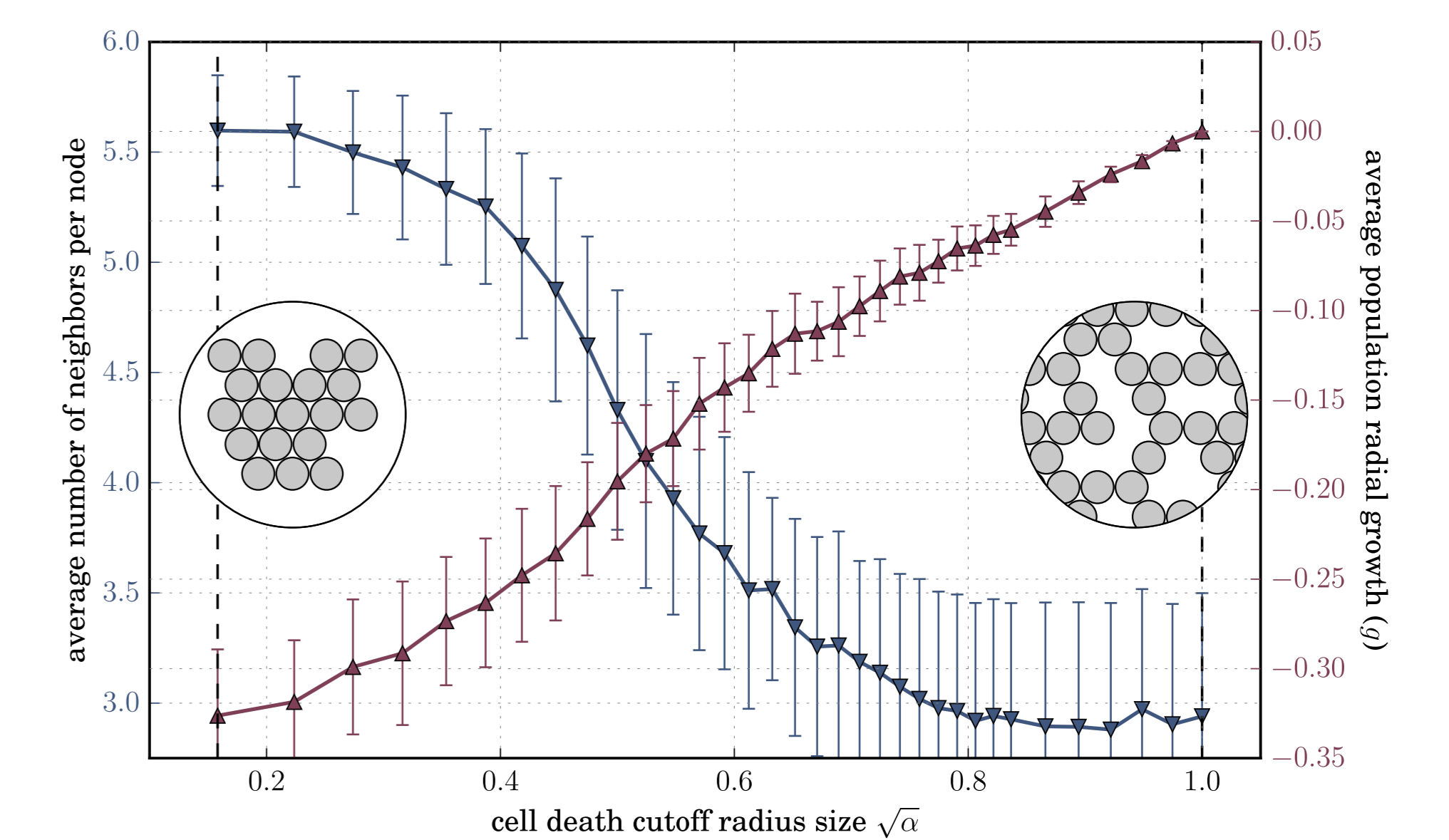
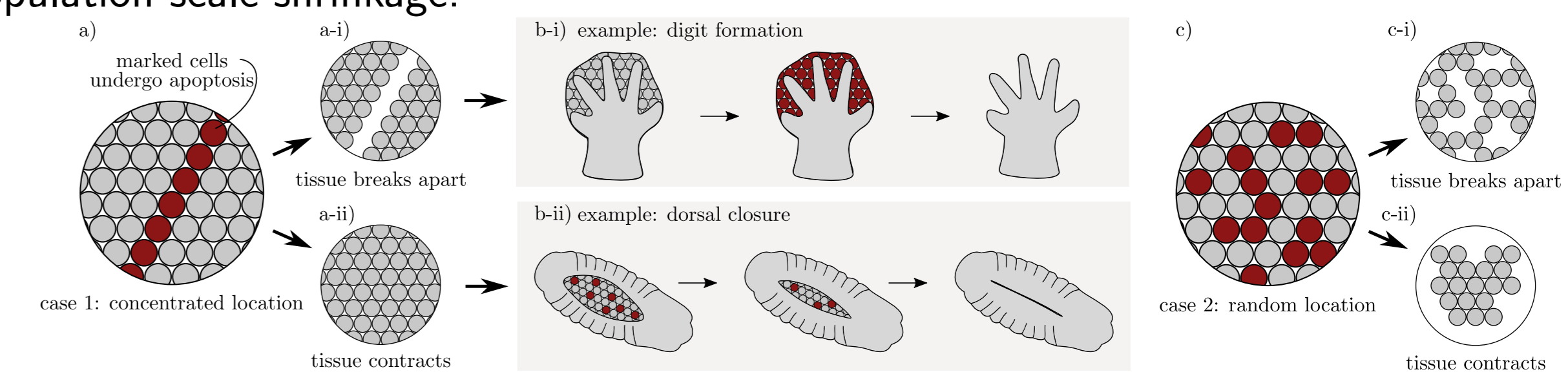


One way to compare different cell growth and division algorithms is to look at the average strain energy density W per cell, and the spatial distribution of stress within a cell population. The upper row of plots shows the average strain energy density W per cell in a growing cell population following different algorithmic rules (200 simulations per line) while the lower row shows the spatial distribution of isochoric stress p (200 simulations per plot).



Apoptotic cell death

Programmed cell death, apoptosis, can occur both naturally and in response to external stimuli. In some cases, apoptosis leads to separation of tissues while in other cases it leads to tissue shrinkage or closure. In this example, we use our computational model to study how the degree of cell shrinkage during apoptosis $\alpha = A_f/A_0$ influences population-scale shrinkage.



In red, the average population growth g , computed from the approximate Jacobian J as $g = \sqrt{J} - 1$, is plotted with respect to $\sqrt{\alpha}$. In blue, the average number of neighbors for each node is plotted with respect to $\sqrt{\alpha}$. Each point represents the mean of 200 simulations where half of the cells undergo apoptosis.

Acknowledgements

- The work is supported by the NSF Graduate Research Fellowship, Grant No. DGE-114747
- Thank you to Claudia Vasquez and Andrew Price from the Dunn Lab at Stanford for the cell images in Fig. 1 · coronal plane T1 MRI: Creative Commons license, user Tdvorak